Journal of Molecular Structure 1048 (2013) 267–273

Contents lists available at SciVerse ScienceDirect

Journal of Molecular Structure

journal homepage: www.elsevier.com/locate/molstruc

Crystal structure and explosive performance of a new CL-20/caprolactam cocrystal

Changyan Guo [a,b], Haobin Zhang [a], Xiaochuan Wang [a], Jinjiang Xu [a], Yu Liu [a], Xiaofeng Liu [a], Hui Huang [a,*], Jie Sun [a,*]

[a] Institute of Chemical Materials, China Academy of Engineering Physics, Mianyang 621900, Sichuan, People's Republic of China
[b] School of Materials Science and Engineering, Southwest University of Science and Technology, Mianyang 621010, Sichuan, People's Republic of China

HIGHLIGHTS

- A novel CL-20/caprolactam cocrystal has been designed and characterized.
- The crystal structure, mechanism and performance are characterized and discussed.
- The formations of cocrystal mainly rely on strong hydrogen bonds interactions.
- The two cocrystal formers can be separated to obtain β-CL-20.
- Provide a good guide for the design of future CL-20 and other explosive cocrystals.

ARTICLE INFO

Article history:
Received 11 January 2013
Received in revised form 10 May 2013
Accepted 15 May 2013
Available online 23 May 2013

Keywords:
Cocrystal
Energetic materials
Structure analysis
Influence factors

ABSTRACT

Co-crystallization is an effective way to improve performance of the high explosive 2,4,6,8,10,12-hexanitrohexaazaisowurtzitane (CL-20). A new CL-20/caprolactam (CPL) cocrystal has been prepared by a rapid solvent evaporation method, and the crystal structure investigations show that the cocrystal is formed by strong intermolecular hydrogen bond interaction. The cocrystal can only be prepared with low moisture content of the air, because water in the air has a profound effect on the cocrystal formation, and it can lead to crystal form conversion of CL-20, but not the formation of cocrystal. The CL20/CPL explosive possess very low sensitivity, and may be used as additive in explosives formulation to desensitize other high explosives.

1. Introduction

Energetic materials (explosives, propellants and pyrotechnics) are used extensively for both civilian and military applications. There are ongoing research programs worldwide to develop new explosives and propellants with higher explosive performance and enhanced insensitivity to thermal or mechanical shock [1]. In recent years, how to improve the explosive performance of existing energetic materials have received a great amount of interest [2–5]. For this purpose, a better approach is to introduce co-crystallization techniques to obtain explosives with excellent comprehensive performance.

Co-crystallization is an effective method to improve the physical and chemical properties of crystalline solid, and it has been widely used in the field of pharmaceutical science [6–8]. By co-crystallization technology, the rate of dissolution, thermal stability and biological activity of the drug can be effectively improved without changing the structure of pharmaceutical active ingredient (API) [9–12]. Currently, researchers also apply this technology to the field of energetic materials as an effective means of changing the density, melting point, decomposition temperature and sensitivity of the explosives. For example, 17 cocrystals of TNT with a range of aromatic or heterocyclic co-formers by Landenberger and Matzger revealed an alteration of key properties including density, melting point and decomposition temperature compared with TNT [13]. Recently, the cocrystals of HMX (1,3,5,7-tetranitro-1,3,5,7-tetrazocane) with a wide variety of co-formers have been reported, which also afford a tremendous reduction in sensitivity compared to pure HMX [14]. Such cases suggest that it is helpful to applied co-crystallization techniques to modulate the physical and chemical properties of existing explosives.

* Corresponding authors. Tel.: +86 0816 2482002 (J. Sun).
E-mail addresses: huangh0816@yahoo.cn (H. Huang), zhuoshisun@sohu.com (J. Sun).

0022-2860
http://dx.doi.org/10.1016/j.molstruc.2013.05.025

CL-20, also called HNIW, is a nitroamine explosive with the formula $C_6H_6N_{12}O_{12}$, primarily used in propellants. It has better oxidizer-to-fuel ratio than the conventional high explosives HMX and RDX [15,16]. However, the high sensitivity usually restricts the storage, transportation, and widely application of CL-20 explosive. In order to improve its safety, a good method is to co-crystallize CL-20 with other insensitive explosive or non-explosive substances to form a new crystal structure [17,18]. Not long ago, Bolton and co-workers prepared a cocrystal of TNT and CL-20, which improves the security of CL-20 while barely reduce the energy [19]. In addition, its density, decomposition temperature and so on have also been modified. In 2012, Bolton et al. reported that a cocrystal of CL-20 and HMX had similar safety properties to HMX, but firing power closer to CL-20 [20]. Although several cocrystals have now been designed to improve the explosive performance of CL-20, the cocrystals is usually difficult to be obtained because of the lack of strong predictable interactions in the chemical structures of its components. The investigation of new CL-20 cocrystal can help to study the formation mechanism and subsequent crystal design and preparation. In addition, the CL-20 cocrystal with non-explosives is needed to obtain explosives with low energy output, which can be used to meet some special requirements, such as smooth blasting, pre-splitting blasting and controlled blasting engineering. In this paper, the non-explosive CPL was chosen to form cocrystal with CL-20, and the cocrystal has been prepared and crystal structure as well as explosive performance are characterized and discussed, which will provide a good guide for the design of future cocrystals of CL-20 and other explosive.

2. Experimental

2.1. Materials

ε-CL-20 was supplied by the Beijing Institute of Technology. Analytical grade caprolactam and anhydrous acetone were provided by Chengdu Institute of Chemical Reagents.

2.2. Cocrystal preparation

Crystallization experiments was conducted by dissolving a molar ratio of 1:5 mixture of ε-CL-20 (4.44 mg) and CPL (5.65 mg) in a minimum amount of anhydrous acetone (dried in the 4A molecular sieve). The solvent was evaporated at 40 °C over a period of several minutes, and a new energetic cocrystal of CL-20/CPL was formed.

2.3. Optical microscopy

Optical micrographs of the crystals were taken under the SK2005A polarization microscope.

2.4. Powder X-ray diffraction (PXRD)

Powder X-ray diffraction patterns were recorded on a Bruker D8 Advance with a Cu Kα radiation (λ = 1.54439 Å), the voltage and current applied were 40 kV and 40 mA, respectively. The data were collected over an angle range from 5° to 50° with a scanning speed of 0.02° per second [21].

2.5. Single crystal X-ray diffraction

The single-crystal X-ray diffraction data of the cocrystal was collected on an Xcalibur, Eos diffractometer. The crystal was kept at 293.15 K during data collection. Crystal structures was solved by direct method using SHELXS, structure solution program using direct method and refined with the SHELXL, refinement package using Least Squares minimisation [22].

2.6. Differential Scanning Calorimeter (DSC)

DSC was performed on a NETZSCH STA 449C Differential Scanning Calorimeter. 1.45–1.78 Mg of samples were placed in aluminium pans and the thermal behaviour of the samples were studied under nitrogen (30.0 ml/min) purge at a heating rate of 10 °C/min over a range from 50 °C to 300 °C [23].

2.7. Infrared spectroscopy (IR)

IR absorption spectra were obtained at a resolution of 4 cm^{-1} using a Nicolet 6700 infrared spectrometer, with each spectrum obtained as the average of 25 individual spectra. Each spectrum was scanned in the range of 400–4000 cm^{-1} with a minimum of six scans [24].

2.8. The drop height at which 50% initiation occurred (H_{50}) and friction sensitivity

The H_{50}: It is based on the varying of the impact energy value in each trial. Depending on the result of previous, the level of impact energy is decreased after ignition for the next trial and increased after "no reaction". In this study we used a 5 kg drop weight, after 25 trials, the level of impact energy with 50% probability of ignition and its standard deviation is determined statistically [25].

The friction sensitivity: The determination of the friction sensitivity was performed referring to the method of WJ1870289 standard and WJ1871280 standard [26]. Dose is 20 mg, pendulum quality is 5 kg, the swing angle is 70° and gauge pressure is 23 MPa.

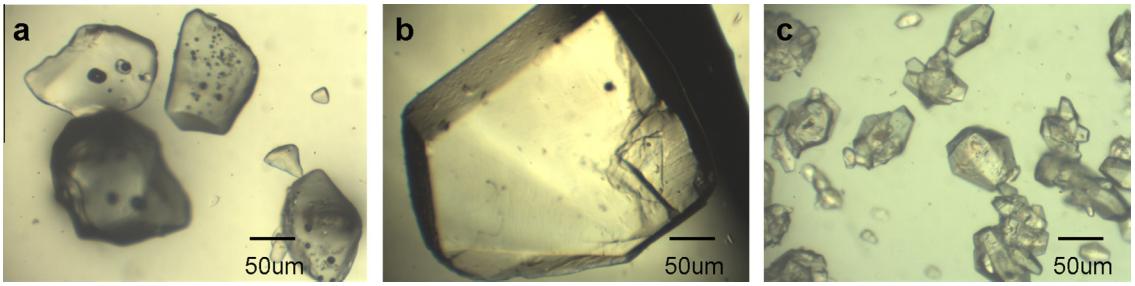

Fig. 1. Microscope images of CPL (a), CL-20/CPL cocrystal (b) and ε-CL-20 (c).

3. Results and discussion

3.1. The microscope images of cocrystal

Macro-morphology of the crystal is a reflection of its microscopic structure, and the crystal morphologies observed under a microscope are shown in Fig. 1. It can been found that the cocrystal was a white tablet-like transparent crystal with well – defined morphology, regular structure, uniform size and smooth surface. All of these differences compared with ε-CL-20 or CPL indicate that the product has a different crystal structure and can be preliminarily implied as cocrystal.

3.2. The DSC results of cocrystal

Differential Scanning Calorimeter is helpful in studies on the thermal behaviour of the cocrystal, and the DSC results are illustrated in Fig. 2. It was evident from the curves that the thermal behaviour of cocrystal is obviously different from their co-formers, and the differences in thermal stability of these substances further suggest the formation of a new cocrystal. The CL-20/CPL cocrystal was found to melt at 89 °C, exhibiting a sharp exothermic process at the temperature of 194 °C. Melting phenomenon of cocrystal appeared in a higher temperature compared with CPL (69 °C), and this phenomenon is consistent with CL-20/TNT cocrystal, which has a higher melting point of 134 °C compared with TNT (80 °C).

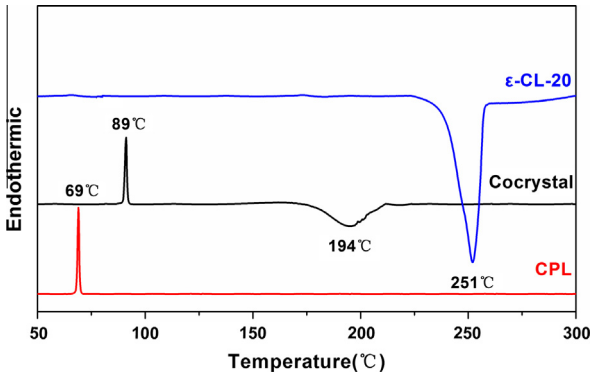

Fig. 2. DSC curves for ε-CL-20, CL-20/CPL cocrystal and CPL.

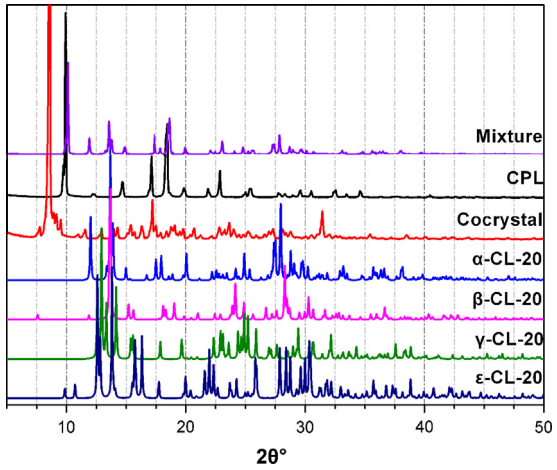

Fig. 3. Comparison of PXRD pattern of the mixture influenced by moisture, CPL, CL-20/CPL cocrystal, α-CL-20, β-CL-20, γ-CL-20 and ε-CL-20.

The different thermal behaviour may be caused by the changes in crystal packing and lattice energy.

3.3. The XRD results of cocrystal

The analysis of XRD approved the formation of cocrystal, and XRD patterns of cocrystal and co-formers are sketched in Fig. 3. The pattern shows that the main diffraction peaks of pure CPL and CL-20 disappeared, replaced by a series of new peaks. A stronger characteristic absorption peak occurs at 2θ angle of 8.6°, which makes the cocrystal easy to be distinguished from pure substances of CPL, α-CL-20, β-CL-20, γ-CL-20 and ε-CL-20 [27]. The cocrystal has a unique X-ray diffraction pattern, which identifies it as a new material rather than product of crystal transformation. The XRD results can been used to further demonstrate the formation of cocrystal.

In addition, the solvent/nonsolvent method, slow solvent evaporation method and rapid solvent evaporation method have been used to obtain desired product. The results of experiments show that the cocrystal can only be prepared by rapid solvent evaporation method, and by other methods only the produce of their mixtures can be obtained (as shown in Fig. 3). These phenomena may result from the water in the air or the solvents, which can lead to crystal form conversion of CL-20, but not the formation of cocrystal, because the formation of α-CL-20 is more advantageous in chemical thermodynamics than that of cocrystal. This phenomenon can be confirmed by the XRD, as can be seen from the graph that the diffraction peak of mixture obtained by other methods is the superposition of CPL and α-CL-20. The conclusion is that the CL-20 cocrystal can only be effectively prepared under the condition of low moisture content of the air, which is helpful to future preparation of other CL-20 cocrystal.

3.4. Structure of the cocrystal

The crystallographic data of CL-20/CPL cocrystal obtained by X-ray single-crystal diffraction meter are presented in Table 1. It reveals that CL-20 and CPL molecules cocrystallizes in a monoclinic system with space group $P2_1/c$ and cell parameters a = 20.8569(19) Å, b = 11.2969(5) Å, c = 23.1262(19) Å and β = 116.613(11)°. It can be seen from Fig. 4a that the cocrystal was formed by the CL-20 and CPL molecules at a molar ratio of 1:5 with a formula weight of 1004.02. The crystal structures viewed along b-axis (Fig. 4b) illustrated that the CL-20 molecules uniformly distributed in CPL molecule to form the desired cocrystal, which contains two different kinds of molecules in a unit cell.

Table 1
Crystal data and structure refinement of CL-20/CPL cocrystal.

Structural parameters	Parameter values
Empirical formula	$C_{36}H_{61}N_{17}O_{17}$
Formula weight	1004.02
Temperature (K)	143.00(10)
Crystal system	Monoclinic
Space group	$P2_1/c$
a (Å)	20.6560(7)
b (Å)	11.1960(3)
c (Å)	23.0104(14)
α (°)	90.00
β (°)	116.866(3)
γ (°)	90.00
Volume (Å^3)	4747.1(4)
Z	4
ρ_{calc} (mg/mm^3)	1.405
Independent reflections	9329[R(int) = 0.0293]
Final R indexes [$I > = 2\sigma(I)$]	R_1 = 0.0433, wR_2 = 0.0985
Final R indexes [all data]	R_1 = 0.0597, wR_2 = 0.1072

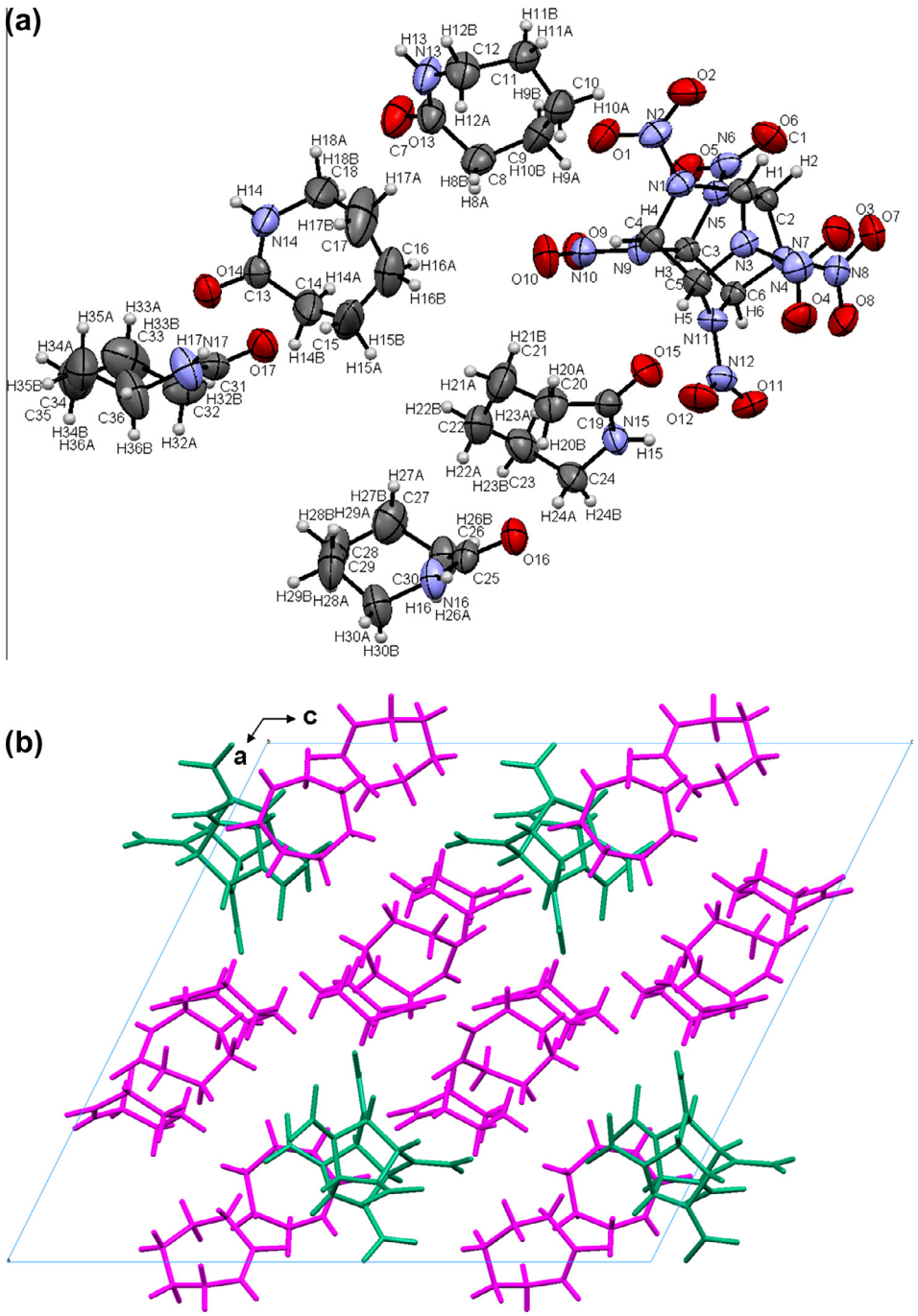

Fig. 4. The cell unit of CL-20/CPL cocrystal, with each atom labelled (a) and the crystal structures viewed along the *b*-axis (b).

In the crystal structure, the strong intermolecular hydrogen bond interactions between nitro groups and adjacent hydrogen are the primary drive forces for the formation of cocrystal, and such intermolecular forces also make contributions to stability of crystal structure [28,29]. These components connected to each other by hydrogen bonds to develop into a huge zigzag network structure which extends into infinity to finish the crystal structure (Fig. 5). The possible hydrogen bond distances and angles found in cocrystal have been listed in Table 2 (the labelled atoms are shown in Fig. 4a). In addition to the hydrogen bonding interaction between caprolactam molecular, such as N15—H15···O10 and N17—H17···O14, the intermolecular interactions between CL-20 and CPL were also found. The formation of CL-20/CPL cocrystal is mainly rely on the strong intermolecular hydrogen bonding interactions to bring the two kind of molecules together, and these interactions are shown in Fig. 6. It can be found that the CL-20 molecules were stabilized by interactions with the CPL molecules around them. Such as the stronger hydrogen bond of C2—H2···O13 between carbonyl group of CPL and hydrogen of CL-20, it is one of the main acting forces for the formation of CL-20/CPL cocrystal, which has a bond distance of 2.481 Å and bond angle of 131.4°.

All of these intermolecular hydrogen bonding interactions are similar with CL-20/TNT cocrystal, and it was stabilized by a number of CH hydrogen bonds each involving nitro group oxygen atoms [19].

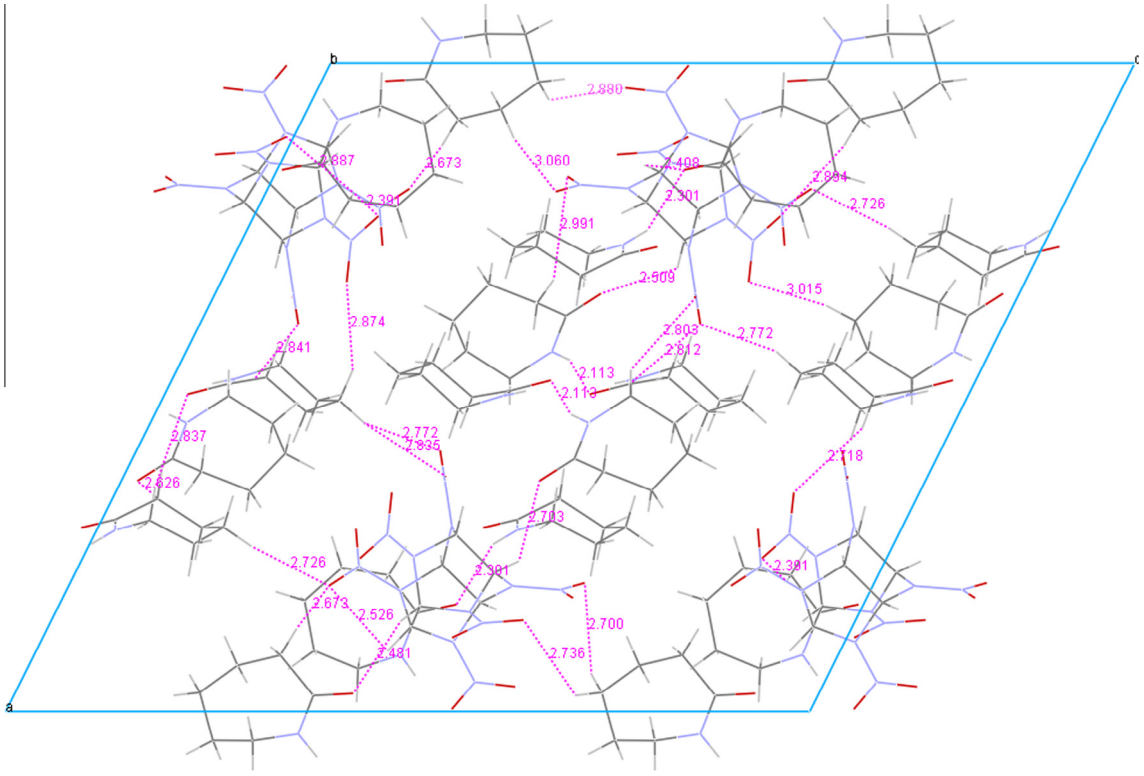

Fig. 5. The CL-20/CPL cocrystal were connected by the possible intermolecular hydrogen bonds to formed a huge zigzag network structure along the *b*-axis.

Table 2
The bond distances and angles of intermolecular hydrogen bonds found in cocrystal.

Interaction	d(Å)	q(°)
N_{15}—$H_{15}\cdots O_{10}$	2.113	158.24
N_{17}—$H_{17}\cdots O_{14}$	2.301	152.79
C_{14}—$H_{14A}\cdots O_7$	2.391	150.97
C_4—$H_4\cdots O_{14}$	2.408	120.98
C_2—$H_2\cdots O_{13}$	2.481	131.43
C_6—$H_6\cdots O_{15}$	2.509	103.46
C_1—$H_1\cdots O_{13}$	2.572	128.15
C_{32}—$H_{32B}\cdots O_{15}$	2.626	178.29
C_8—$H_{8A}\cdots O_3$	2.673	148.08
C_{10}—$H_{10B}\cdots O_9$	2.700	135.70
C_3—$H_3\cdots O_{15}$	2.703	99.32
C_{26}—$H_{26A}\cdots O_8$	2.718	150.92
C_{34}—$H_{34A}\cdots O_3$	2.726	157.13
C_{10}—$H_{10A}\cdots O_5$	2.736	121.36
C_{28}—$H_{28B}\cdots O_{11}$	2.772	139.79
C_{24}—$H_{24B}\cdots O_{12}$	2.803	117.37
C_{24}—$H_{24A}\cdots O_{11}$	2.812	123.05
C_{28}—$H_{28B}\cdots O_{12}$	2.835	167.26
C_{36}—$H_{36B}\cdots O_{16}$	2.837	169.22
C_{26}—$H_{26B}\cdots O_{11}$	2.841	116.46
C_{28}—$H_{28A}\cdots O_8$	2.874	148.23
C_{10}—$H_{10B}\cdots O_1$	2.880	131.98
C_{14}—$H_{14A}\cdots O_6$	2.887	119.34
C_8—$H_{8A}\cdots O_7$	2.894	136.09
C_{20}—$H_{20A}\cdots O_{10}$	2.991	137.07
C_{22}—$H_{22B}\cdots O_8$	3.015	150.27
C_9—$H_{9A}\cdots O_9$	3.060	110.02

3.5. The IR results of cocrystal

FTIR spectroscopy is normally used for the phase determination of CL-20 and works very well in determination of the predominant phase [30,31] and the changes caused by intermolecular hydrogen bond are relatively apparent in the infrared spectrum [32].

Fig. 7 shows that several regions are highly sensitive to the structure changes of the cocrystal in the IR spectra, and part of characteristic absorption peak of the group offset significantly. It can be concluded from the chart that a group of low intensity bands assigned to the C—H stretching of CL-20 shifted from the region of 3045–3013 cm^{-1} to 3049–3030 cm^{-1}. While, C—H stretching vibration of CPL increased from the region of 2929–2856 cm^{-1} to 2934–2861 cm^{-1}, and the C=O stretching vibration increased from 1655 cm^{-1} to 1668 cm^{-1}. Those phenomena may be caused by the hydrogen bond interactions involved in cocrystal formation. Among three stretching of the nitramine group of CL-20, $^{as}(NO_2)$ (antisymmetric stretching vibration), $^{s}(NO_2)$ (symmetric stretching vibration), (N—N), only $^{as}(NO_2)$ can be considered as approximately characteristic and used in analytical investigations [33]. In CL-20/CPL cocrystal, a group of frequencies located near 1632–1566 cm^{-1} are assigned to asymmetrical NO_2 stretching of CL-20. It reduced to 1599–1561 cm^{-1} due to the interactions with CPL, and conversely, the NH stretching vibration increased from the region of 3213–3297 cm^{-1} to 3285–3293 cm^{-1} for the same reason. The symmetrical NO_2 stretching modes mixed with other vibrations located in the same region, especially with CH-bonds.

All the changes in infrared absorption due to electron cloud density variations of functional groups that can form intermolecular hydrogen bond with their neighbouring molecule. So, this phenomenon also indicated that the intermolecular hydrogen bond was the primary forces driving cocrystal formation.

3.6. Cocrystal properties

Properties are important factors to evaluate the application value of explosives [34]. The CL-20/CPL cocrystal is a kind of energetic material with relatively low density of 1.405 g/cm^3, which indicate that the CL-20/CPL cocrystal may have low energetic properties. However, the adding of non-explosive substance may make

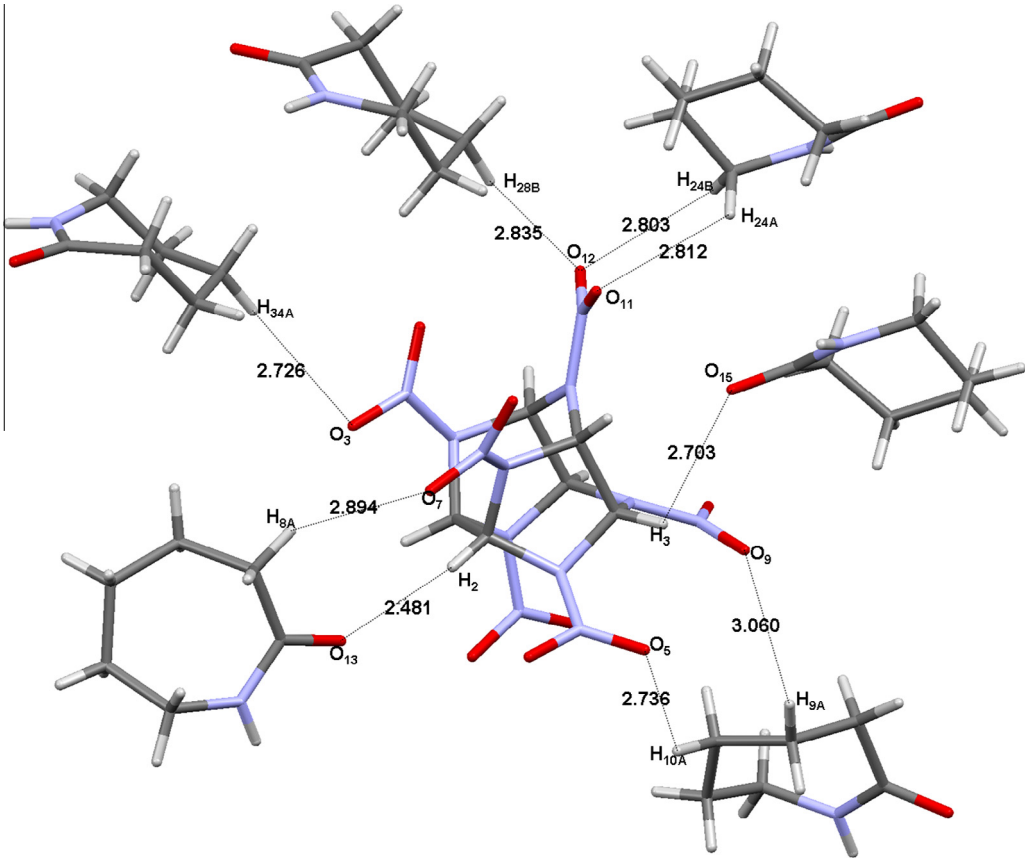

Fig. 6. The intermolecular hydrogen bonds between CL-20 and CPL molecule found in cocrystal.

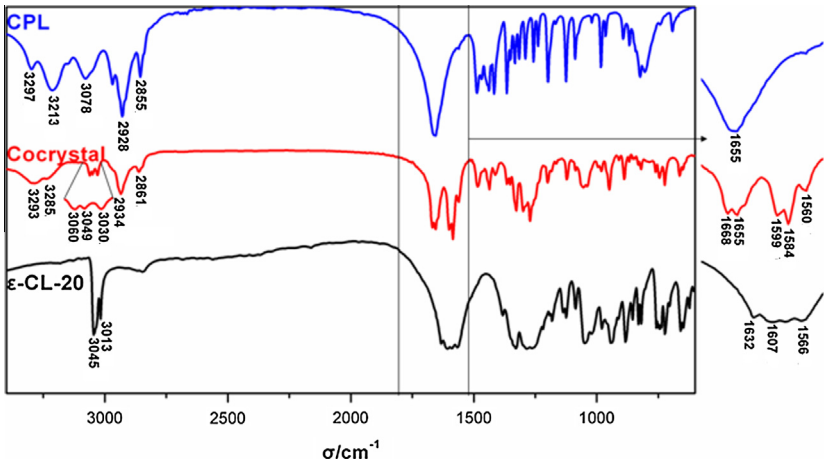

Fig. 7. IR spectra of CPL, CL-20/CPL cocrystal and ε-CL-20.

the cocrystal with lower sensitivity, and can be applied to some other places, which has lower requirements of explosive energy. To analyze the security, the impact sensitivity and friction sensitivity of cocrystal was studied. The results revealed its insensitive nature towards mechanical stimuli, with a friction sensitivity of 0% (No explosion occurred in the test conditions) and H_{50} (50% explosion characteristics of drop height) of 84 cm, which shows a satisfactory security than that of CL-20 (H_{50} = 16 cm).

Other than above, separation test of cocrystal has been made by means of different solubility. 0.5 g cocrystal was added to 10 ml chloroform and sonication for 10 min to obtain the β-CL-20 after filtration and drying. Particles of the crystal were examined under a microscope, and it shows that the β-CL-20 with a crystal particle size of about 5 μm or so was successfully received, and the results were confirmed by XRD. This implied that the β-CL-20 crystals with a relatively small particle size can be obtained by separation test of CL-20/CPL cocrystal, and it may be a new way to prepare the micronized CL-20.

4. Conclusion

A novel CL-20/CPL cocrystal with the molar ratio of 1:5 has been discovered and characterized. The formation of cocrystal is mainly

influenced by strong intermolecular hydrogen bond interactions, and these new interactions make it has unique crystal orientation and spatial arrangement compared with its components. The cocrystal has a lower melting point and density, but better security, wihch is very advantageous in some blasting engineering, and it also proved that the performance of energetic materials can be modified by cocrystallization to get better comprehensive explosives. In addition, we found that the absolute dry condition is needed to prevent the conversion of crystal form of CL-20 during the cocrystal preparation, and the cocrystal can only be prepared by rapid solvent evaporation method, which is useful to future design and preparation of other CL-20 cocrystal. And also, the β-CL-20 crystals with a relatively small particle size can be obtained by separation test of CL-20/CPL cocrystal, and a new way is carried out for designing and preparing of micronized CL-20.

Acknowledgements

This work is supported by the National Science Foundation (No. 11076002); the Science Foundation of China Academy of Engineering Physics (No. 2012A0302013) and the Young Talents Cultivation Fund of Institute of Chemical Materials, China Academy of Engineering Physics (No. 626010946), China.

References

[1] P.F. Pagoria, G.S. Lee, A.R. Mitchell, R.D. Schmidt, Thermochim. Acta 384 (2002) 187–204.
[2] Z.A. Dreger, Y.M. Gupta, J. Phys. Chem. A 114 (2010) 8099, http://dx.doi.org/10.1021/jp105226s.
[3] F.P.A. Fabbiani, C.R. Pulham, Chem. Soc. Rev. 35 (2006) 932, http://dx.doi.org/10.1039/B517780B.
[4] J. Evers, T.M. Klapötke, P. Mayer, G. Oehlinger, J. Welch, Inorg. Chem. 45 (2006) 4996, http://dx.doi.org/10.1021/ic052150m.
[5] W.C. McCrone, Anal. Chem. 22 (1950) 1225.
[6] P. Sanphui, S.S. Kumar, A. Nangia, Cryst. Growth Des. 12 (2012) 4588, http://dx.doi.org/10.1021/cg3004245.
[7] N. Shan, M.J. Zaworotko, Drug Discov. Today 13 (2008) 440, http://dx.doi.org/10.1016/j.drudis.2008.03.004.
[8] S. Basavoju, D. Boström, P.S. Velaga, Cryst. Growth Des. 6 (2006) 2699, http://dx.doi.org/10.1021/cg060327x.
[9] I. Miroshnyk, S. Mirza, N. Sandler, Expert Opin. Drug Deliv. 6 (2009) 333, http://dx.doi.org/10.1517/17425240902828304.
[10] Z.Z. Wang, J.M. Chen, T.B. Lu, Cryst. Growth Des. 12 (2012) 4562, http://dx.doi.org/10.1021/cg300757k.
[11] V.K. Srirambhatla, A. Kraft, S. Watt, A.V. Powell, Cryst. Growth Des. 12 (2012) 4870, http://dx.doi.org/10.1021/cg300689m.
[12] R. Chadha, A. Saini, D.S. Jain, P. Venugopalan, Cryst. Growth Des. 12 (2012) 4211, http://dx.doi.org/10.1021/cg3007102.
[13] K.B. Landenberger, A.J. Matzger, Cryst. Growth Des. 10 (2010) 5341, http://dx.doi.org/10.1021/cg101300n.
[14] K.B. Landenberger, A.J. Matzger, Cryst. Growth Des. 12 (2012) 3603–3609, http://dx.doi.org/10.1021/cg3004245.
[15] N.V. Latypov, U. Wellmar, P. Goede, Org. Process Res. Dev. 4 (2000) 156, http://dx.doi.org/10.1021/op990097d.
[16] T.P. Russell, P.J. Miller, G.J. Piermarini, S. Block, J. Phys. Chem. 97 (1993) 1993, http://dx.doi.org/10.1021/j100111a043.
[17] Y.T. Lapina, A.S. Savitskii, E.V. Motina, N.V. Bychin, A.A. Lobanova, N.I. Golovin, Russ. J. Appl. Chem. 82 (2009) 1821, http://dx.doi.org/10.1134/S1070427209100140.
[18] I.A.D. Millar, E.H. Maynard-Casely, CrystEngComm 14 (2012) 3742, http://dx.doi.org/10.1039/c2ce05796d.
[19] O. Bolton, A.J. Matzger, Angew. Chem. Int. Ed. 50 (2011) 8960, http://dx.doi.org/10.1002/anie.201104164.
[20] O. Bolton, L.R. Simke, P.F. Pagoria, A.J. Matzger, Cryst. Growth Des. 12 (2012) 4311, http://dx.doi.org/10.1021/cg3010882.
[21] X.Y. Shu, Y. Tian, G.B. Song, H.B. Zhang, B. Kang, C.Y. Zhang, J. Sun, J. Mater Sci. 46 (2011) 2536, http://dx.doi.org/10.1007/s10853-010-5105-0.
[22] J. Marcotrigiano, A.C. Gingras, N. Sonenberg, S.K. Burley, Cell 89 (1997) 951, http://dx.doi.org/10.1016/S0092-8674(00)80280-9.
[23] G.V. Frederick, A.V. Joseph, C. Manisha, S.C. Jacalyn, S. Mark, E.B. Maria, J. Mol. Struct. 932 (2009) 16, http://dx.doi.org/10.1016/j.molstruc.2009.05.035.
[24] C.K. Amal, D. Subin, K.B. Kamal, S. Eringathodi, J. Mol. Struct. 985 (2011) 361, http://dx.doi.org/10.1016/j.molstruc.2010.11.022.
[25] Y.C. Li, W. Liu, S.P. Pang, Molecules 17 (2012) 5040, http://dx.doi.org/10.3390/molecules17055040.
[26] GJB 5891.24-2006, Test Method of Loading Material for Initiating Explosive Device, Part 24: Friction Sensitivity Test, Commision on Science, Technology, and Industry for National Defense, 2006.
[27] P. Goede, N.V. Latypov, H. östmark, Propellants Explos. Pyrotech. 29 (2004) 205, http://dx.doi.org/10.1002/prep.200400047.
[28] R.K.R. Jetti, R. Boese, P.K. Thallapally, G.R. Desiraju, Cryst. Growth Des. 3 (2003) 1033, http://dx.doi.org/10.1021/cg034141z.
[29] C. Näther, C. Arad, H. Bock, Acta. Cryst. C 53 (1997) 76, http://dx.doi.org/10.1107/S0108270196011766.
[30] Y. Kholod, S. Okovytyy, G. Kuramshina, M. Qasim, L. Gorb, J. Leszczynski, J. Mol. Struct. 843 (2007) 14, http://dx.doi.org/10.1016/j.molstruc.2006.12.031.
[31] A.E. Fogel'zang, B.S. Svetlov, V.Y. Adzhemyan, S.M. Kolyasov, O.I. Sergienko, S.M. Petrov, Combust. Explo. Shock Waves 12 (1976) 732–740, http://dx.doi.org/10.1007/BF00740743.
[32] Y.B. Che Man, G. Setiowaty, Food Chem. 66 (1999) 109. org/10.1016/S0308-8146(98)00254-4.
[33] M. Qasim, H. Fredrickson, P. Honea, J. Furey, J. Leszczynski, S. Okovytyy, J. Szecsody, Y. Kholod, SAR QSAR Environ. Res. 16 (2005) 495, http://dx.doi.org/10.1080/10659360500320453.
[34] N.R. Goud, S. Gangavaram, K. Suresh, S. Pal, S.G. Manjunatha, S. Nambiar, A. Nangia, J. Pharm. Sci. 101 (2012) 664–680, http://dx.doi.org/10.1002/jps.22805.